Supplementary material for

Extreme tolerance to chromosomal restructuring and male-linked B chromosome inheritance in Neotropical vertebrate model

Journal: BMC Biology Direct

Tomáš Pavlica, Ahmed Al-Rikabi, Tomáš Dvořák, Vendula Bohlen Šlechtová, Niklas Padutsch, Thomas Liehr*, Petr Ráb, Milena Ferreira, Eliana Feldberg, Marcelo de Bello Cioffi, Alexandr Sember*

* Correspondence:

Thomas.Liehr@med.uni-jena.de; Jena University Hospital, Friedrich Schiller University, Institute of Human Genetics, Jena, Germany

sember@iapg.cas.cz; Institute of Animal Physiology and Genetics, Czech Academy of Sciences, Liběchov, Czech Republic

The PDF file includes:

Table S1 DNA sequences generated de novo or downloaded from GenBank for the purpose of phylogenetic reconstruction

Species		Individual code	GenBank accession numbers		
			CO I	MYH 6	RAG 1
Bunocephalus aloikae		BAL 1	PP335561	PP335596	PP335631
		BAL 2*	PP335572	PP335607	PP335642
		BAL 3*	PP335576	PP335611	PP335646
		BAL 4*	PP335577	PP335612	PP335647
		BAL 5*	PP335578	PP335613	PP335648
		BAL 6	PP335579	PP335614	PP335649
		BAL 7*	PP335580	PP335615	PP335650
		BAL 8*	PP335581	PP335616	PP335651
		BAL 9*	PP335582	PP335617	PP335652
		BAL 10*	PP335562	PP335597	PP335632
		BAL 11	PP335563	PP335598	PP335633
		BAL 12	PP335564	PP335599	PP335634
		BAL 13	PP335565	PP335600	PP335635
		BAL 14*	PP335566	PP335601	PP335636
		BAL 15	PP335567	PP335602	PP335637
		BAL 16*	PP335568	PP335603	PP335638
		BAL 17	PP335569	PP335604	PP335639
		BAL 18	PP335570	PP335605	PP335640
		BAL 19*	PP335571	PP335606	PP335641
		BAL 20*	PP335573	PP335608	PP335643
		BAL 21*	PP335574	PP335609	PP335644
		BAL 22	PP335575	PP335610	PP335645
		BAL C1?	PP335583	PP335618	PP335653
		BAL C2?	PP335584	PP335619	PP335654
		BAL C3?	PP335585	PP335620	PP335655
		BAL C4?	PP335586	PP335621	PP335656
		BAL C5?	PP335587	PP335622	PP335657
		BAL C6?	PP335588	PP335623	PP335658
		BAL C7?	PP335589	PP335624	PP335659
Bunocephalus coracoideus		BCO M1*	PP335590	PP335625	PP335660
		BCO 3	PP335591	PP335626	PP335661
		BCO F1*	PP335592	PP335627	PP335662
		BCO 5	PP335593	PP335628	PP335663
		BCO 78	PP335594	PP335629	PP335665
		BCO 79	PP335595	PP335630	PP335664
Comparative GenBank material					
Bunocephalus aleuropsis	1	INPA43490_t10813	MF489396	MF489550	MF489458
	2	ANSP197608_t11335	MF489397	MF489552	MF489460
	3	LBP1850_LBP13507	MF489406	MF489545	MF489453
	4	LBP1850_LBP13508	MF489407	MF489546	MF489454
	5	LBP4128_LBP23632	MF489408	MF489547	MF489455
	6	LBP4128_LBP23633	MF489409	MF489548	MF489456
	7	UFRO-IUncat.Gen6637	MF489410	MF489543	MF489451
	8	UFRO-I13443_Gen6728	MF489411	MF489544	MF489452
	9	INHS54702_t11112	MF489412	MF489551	MF489459
	10	INHS54702_t4935	MF489413	MF489549	MF489457
Bunocephalus aloikae	1	ANSP197190_LBP18640	MF489388	MF489615	MF489461
	2	LBP10162_LBP47569	MF489389	MF489553	MF489462
	3	MHNG2671.0081_SU05_560	MF489390	MF489554	MF489464
	4	MHNG2671.0081_SU05_558	MF489391	MF489614	MF489463

	5	MHNG2671.026_SU05_530	MF489392	MF489555	MF489465
	6	ANSP198869_t12946	-	MF489556	MF489466
Bunocephalus amaurus	1	ANSP189095_t1294	MF489400	MF489561	MF489438
	2	MHNG2700.0024_GF07_101	MF489401	MF489557	MF489467
	3	MHNG2700.0025_GF07_225	MF489402	MF489558	-
	4	MHNG2700.0236_GF07_255	MF489403	MF489559	-
	5	MHNG2700.0237_GF07_256	MF489404	MF489560	-
	6	ANSP180022_t11069	MF489405	MF489562	MF489468
	7	INPA-ICT 052187__11842	MF416200	-	-
	8	INPA-ICT 052187__11845	MF416202	-	-
Bunocephalus coracoideus	1	LBP4067_LBP22961	MF489417	-	MF489472
	2	LBP4067_LBP22962	MF489418	MF489567	MF489473
	3	ANSP192024_t4673	MF489419	MF489572	MF489480
	4	ANSP178215_t1683	MF489420	MF489570	MF489477
	5	INHS53737_t4643	MF489421	MF489571	MF489479
	6	ANSP179019_t2209	MF489422	-	MF489478
	7	INHS43560_t4880	MF489423	MF489573	MF489481
	8	LBP6974_LBP34016	MF489424	MF489569	MF489475
	9	LBP6974_LBP34015	MF489425	MF489568	MF489474
	10	INPA-ICT 053204_11617	MF416164	-	-
	11	INPA-ICT 053204_12518	MF416165	-	-
	12	INPA-ICT 053205_11872	MF416168	-	-
	13	INPA-ICT 053205_11873	MF416169	-	-
	14	INPA-ICT 052188_11824	MF416173	-	-
	15	INPA-ICT 052188_11829	MF416176	-	-
	16	INPA-ICT 052185_11740	MF416184	-	-
	17	INPA-ICT 052185_11744	MF416185	-	-
Bunocephalus colombianus	1	STRI142	-	MF489565	MF489471
	2	STRI1576	-	MF489566.2	-
Bunocephalus doriae	1	MCP25223_UR053	MF489393	MF489577	-
	2	UFRGS16333_TEC2771	-	MF489576	MF489484
	3	UFRGS12357_TEC616	-	MF489575	MF489483
	4	ANSP184211_t4807	-	MF489574	MF489482
	5	MCP<BRA>:25223	MF595228	-	MF595298
Bunocephalus larai	1	LBP11715_LBP59903	MF489394	MF489579	MF489486
	2	LBP11730_LBP59963	MF489395	MF489580	MF489487
	3	LBP11715_LBP59902	-	MF489578	MF489485
Bunocephalus minerim	1	UFRGS11374_TEC1212	MF489398	MF489581	MF489488
	2	MCP49168_z01	MF489399	MF489582	MF489489
Bunocephalus verrucosus	1	CU 91989	EU490846	EU490958	-
	2	LBP4310_LBP23988	MF489426	-	MF489492
	3	MCP46203_XXIV-94	MF489427	MF489588	MF489496
	4	AUM35819_t11209	MF489428	MF489587	MF489495
	5	LBP4310_LBP23989	MF489429	-	MF489493
	6	ANSP180015_t11036	MF489430	MF489586	MF489494
Bunocephalus sp. *negro*	1	LBP6895_LBP33237	MF489415	MF489583	MF489490
	2	LBP6895_LBP33478	MF489416	MF489584	-
	3	INPA-ICT 053204_12163	MF416167	-	-
Bunocephalus sp. *orinoco*		AUM43375_t9383	MF489414	MF489585	MF489491
Outgroup					
Aspredo aspredo		MHNG2608.035_GF99_034	MF489355	MF489540	MF489447
Additional sequences for divergence time estimation					
Hoplomyzon sexpapilostoma		CU 82559	EU490843	DQ492592	-

Micromyzon akamai	ANSP:FISH:182777	EU490844	DQ492644	-
Pseudobunocephalus iheringii	MCP25226_WAS061	MF489371	MF489602	MF489515
Pterobunocephalus dolichurus	ANSP182745_t1806	MF489433	MF489607	MF489524
Xyliphius magdalenae	ANSP192845_t4489	MF489382	MF489609	MF489527
Cetopsis coecutiens	ANSP182760_t1833	MF489362	MF489619	MF489497
Clarias batrachus		JF280822	-	DQ492568
Clarias fuscus		NC_023941	-	JN020121
Heteropneustes fossilis		OR801155	-	-
Franciscodoras marmoratus	LBP 272 Tag 4193	KC555610	KC555741	MF595310
Nemadoras humeralis	ANSP:FISH:182596	KC555649	KC555771	MF595323
Rhynchodoras woodsi	ANSP:FISH:181042	KC555694	KC555811	MF595330
Trachydoras steindachneri	MUSM33868_AP153	MF489363	MF489608	MF489525
Corydoras stenocephalus	T12839	-	-	KP960365

* = individuals used for cytogenetic experiments; “?” denotes individual F27 which was selected from the C1–C7 cohort. Given the high phylogenetic similarity of these individuals, specific identification within this group was deemed unnecessary

Table S2 Primer sequences used for the phylogenetic analysis

Locus	Primer name	Primer sequence (5’ - 3’)	Reference
CO I	Fish F1	TCA ACC AAC CAC AAA GAC ATT GGC AC	[1]
	Fish R1	*TAG ACT TCT GGG TGG CCA AAG AAT CA*	[1]
RAG 1	RAG-F354	CAG AGC ATG AGG TVC AGG GAG ATC T	[2]
	RAG-R1333	*GTC AAA CAC ACA GAC TTC ACA TC*	[2]
MYH 6	myh6-F507	GGA GAA TCA RTC KGT GCT CAT CA	[3]
	myh6-R1322	*CTC ACC ACC ATC CAG TTG AAC AT*	[3]
	myh6-F459	CAT MTT YTC CAT CTC AGA TAA TGC	[3]
	myh6-R1325	*ATT CTC ACC ACC TCC AGT TGA A*	[3]

Table S3 Overview of the most crucial cytogenetic results in all individuals of *Bunocephalus aloikae* individuals

Individual	2n (A+B)	BAL-tetr signals	BAL-meta signals	Male specific CGH (A+B)	5S rDNA var. I signals	18S rDNA signals	CMA_3+ signals	ITS
BAL ♂4	48 (48+0)	4	2	2	6	2	10	2
BAL ♂5	50 (49+1)	5	3	2+1	6	2	11	2
BAL ♂7	51 (50+1)	4	3	2+1	5	3	12	2
BAL ♂9	49 (49+0)	4	2	2	6	2	10	NO
BAL ♂10	50 (48+2)	4	3	2+2	5	4	10	1
BAL ♂16	49 (49+0)	4	3	2	6	2	9	2
BAL ♂19	50 (50+0)	4	2	2	6	2	±10	2
BAL ♂20	50 (50+0)	4	3	1	6	2	10	1
BAL ♀2	49 (49+0)	5	2	2	6	2	11	2
BAL ♀3	50 (50+0)	4	4	NO	6	2	11	2
BAL ♀8	47 (47+0)	4	3	NO	5	2	11	3
BAL ♀14	49 (49+0)	4	3	NO	6	2	10	1
BAL ♀21	49 (49+0)	4	4	NO	5	2	10	1
BAL ♀27	49 (49+0)	5	6	NO	6	2	10	3

In the brackets below 2n, the numbers represent standard (A) chromosomes + supernumerary (B) chromosomes. The number of BAL-tetr and BAL-meta WCP signals do not include the overlapping signals on B chromosomes (see the main text for more information). Male-specific CGH describes the number of regions preferentially stained by the male genomic probe. 18S rDNA signals include also those located on B chromosomes (one in BAL M7, two in BAL M10). ITS = interstitial telomeric sequence.

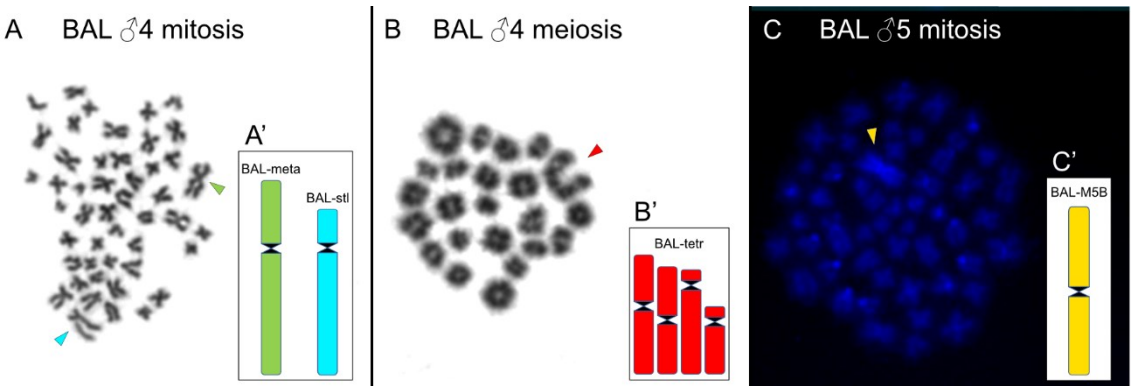

Fig. S1 Chromosome spreads from *Bunocephalus aloikae* males M4 and M5. The arrows mark the microdissected objects for WCP probes. (A) mitotic metaphase; blue arrow points on a single subtelocentric chromosome without homolog used for BAL-stl; green arrowhead marks single large metacentric chromosome used for BAL-meta. (B) Meiotic metaphase I. Red arrowhead points on a tetravalent used for BAL-tetr. (C) mitotic metaphase; yellow arrowhead marks large metacentric chromosome used for BAL-M5B.

Fig. S2 Bayesian phylogenetic tree reconstructed using MrBayes from a concatenated dataset. Node values indicate Bayesian posterior probabilities.

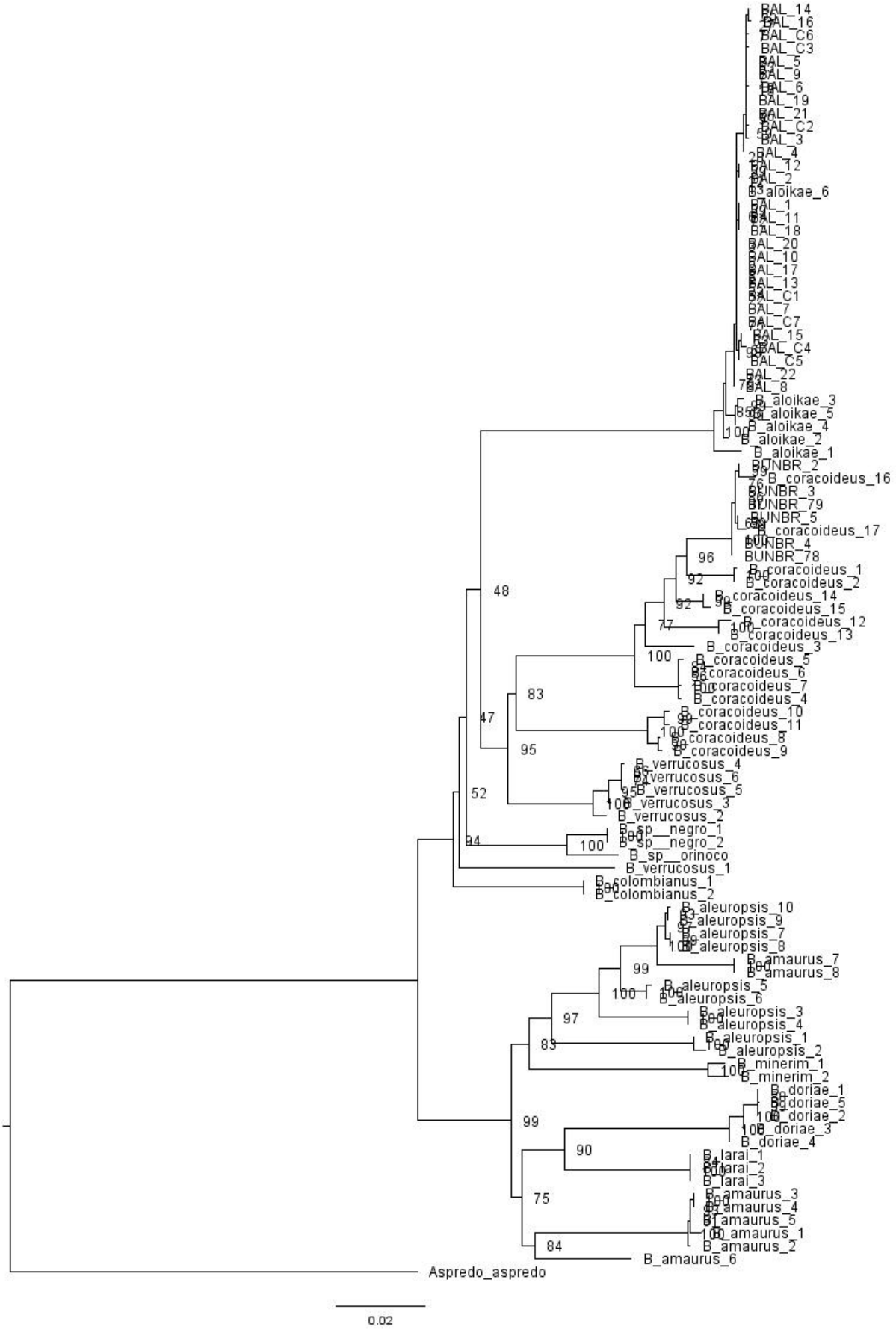

Fig. S3 Maximum likelihood phylogenetic tree inferred using IQ-TREE from a concatenated dataset. Node labels indicate ultrafast bootstrap support values.

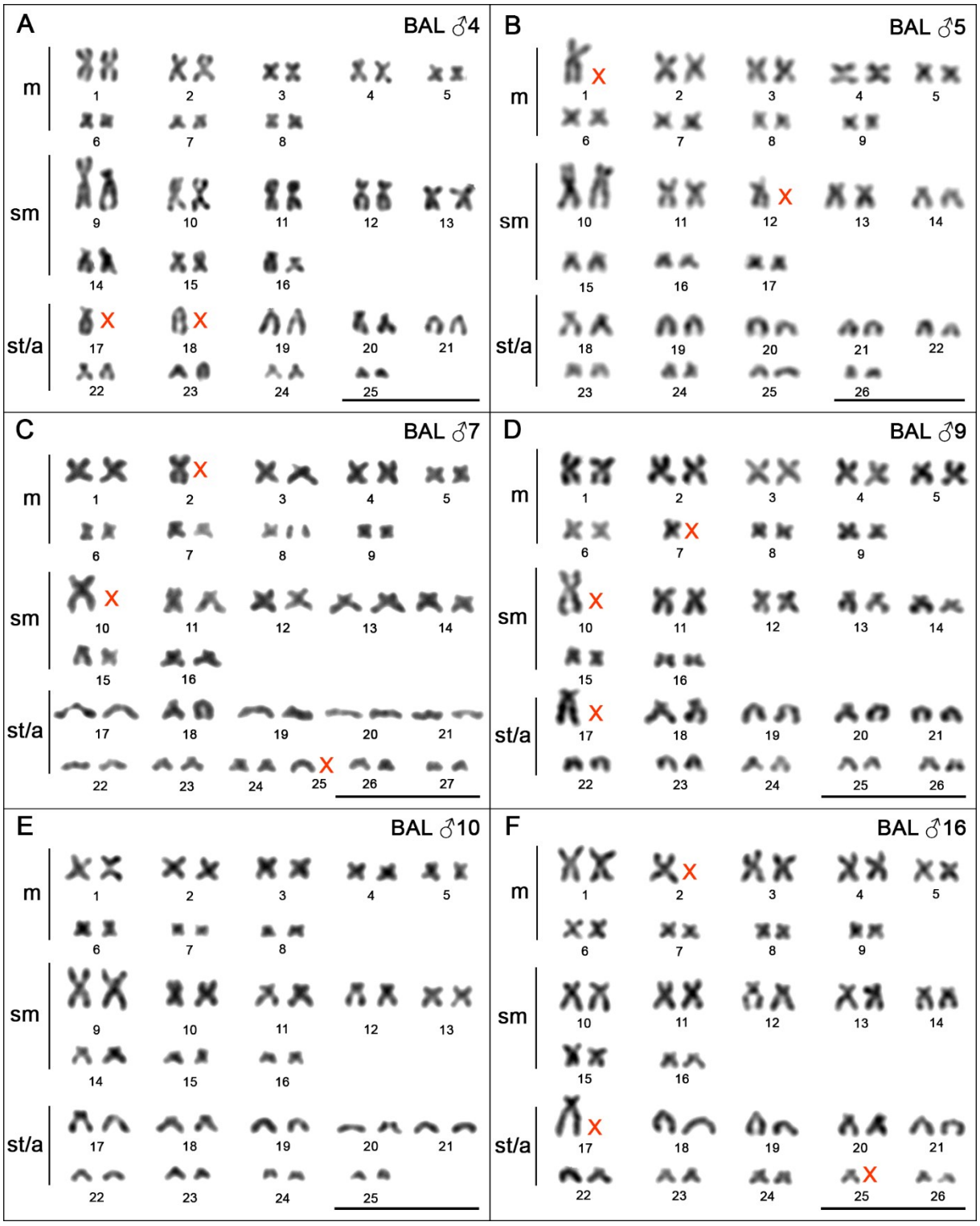

Fig. S4 Karyotypes of *Bunocephalus aloikae* males (part I) after Giemsa staining. m = metacentric chromosome, sm = submetacentric chromosome, st/a = subtelocentric-to-acrocentric chromosome.

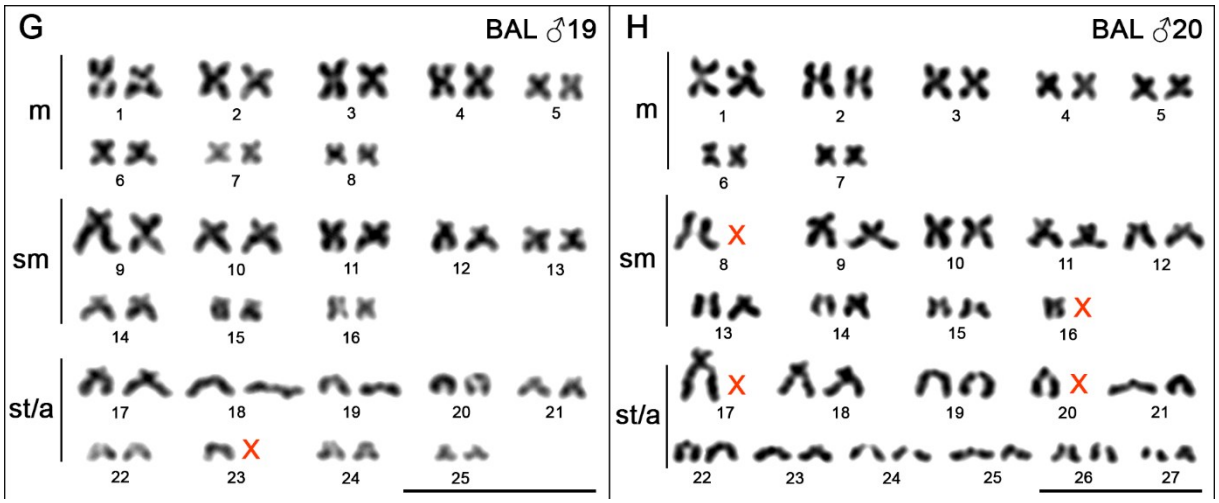

Fig. S5 Karyotypes of *Bunocephalus aloikae* males (part II) after Giemsa staining. m = metacentric chromosome, sm = submetacentric chromosome, st/a = subtelocentric-to-acrocentric chromosome.

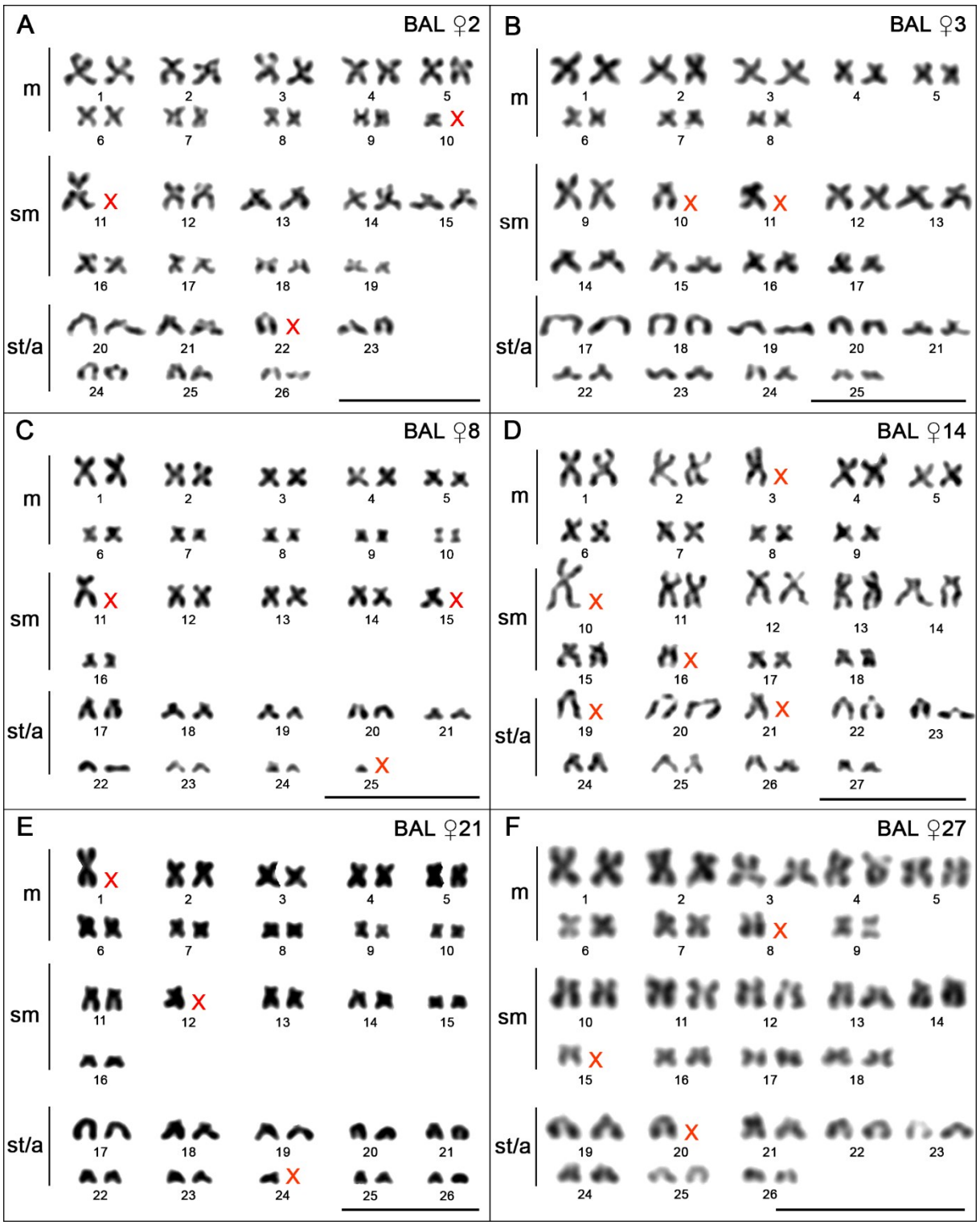

Fig. S6 Karyotypes of *Bunocephalus aloikae* females after Giemsa staining. m = metacentric chromosome, sm = submetacentric chromosome, st/a = subtelocentric-to-acrocentric chromosome.

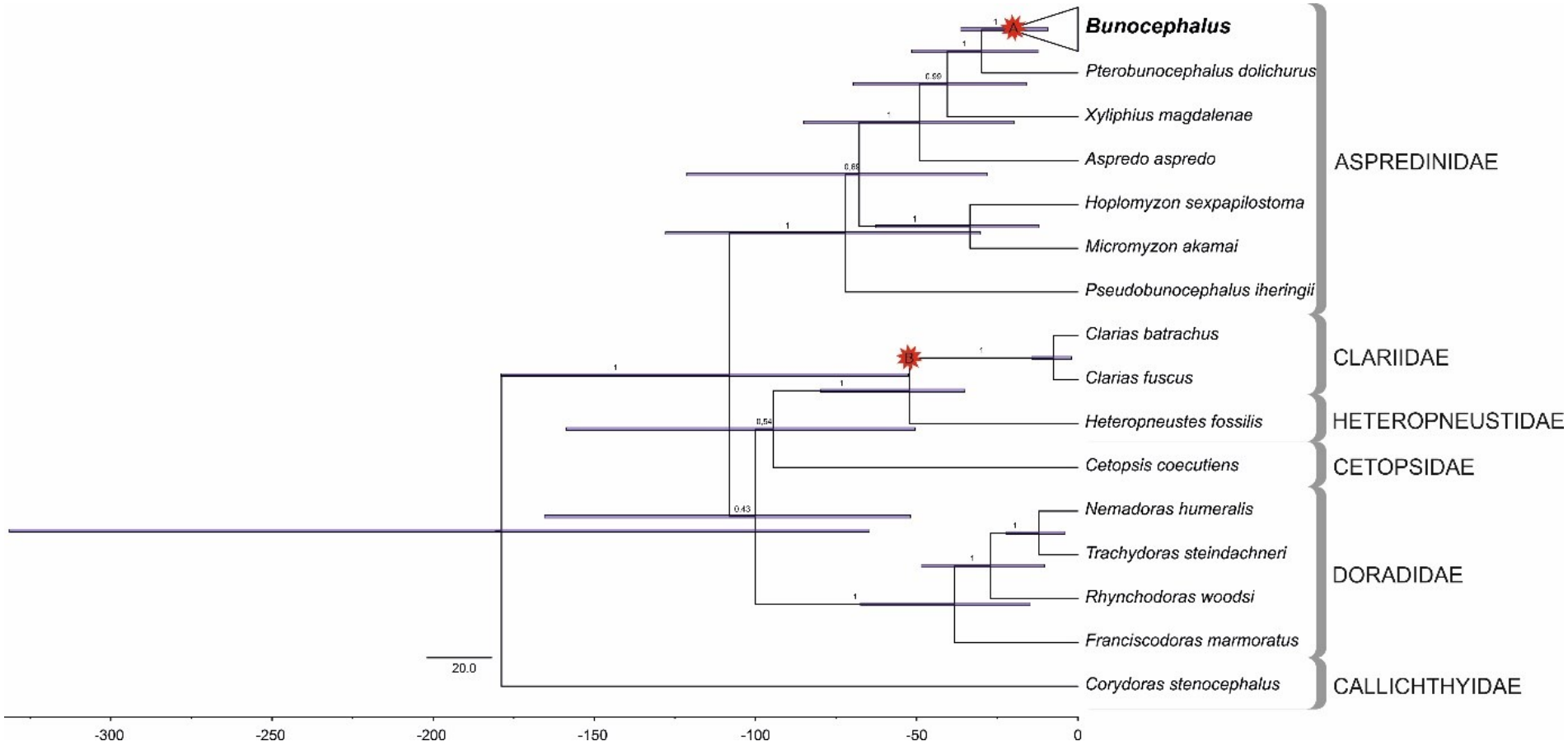

Fig. S7 Maximum clade credibility (MCC) tree inferred from Bayesian divergence time analysis of the concatenated dataset in BEAST2, including *Bunocephalus* and extended outgroup taxa. The analysis was performed under a Birth–Death tree prior with fossil-based calibrations. Numbers at branches indicate posterior probabilities, and blue bars represent 95% highest posterior density (HPD) intervals of node ages. Red stars denote calibration points: (A) crown calibration of the genus *Bunocephalus*, based on the oldest reliably assigned fossil record of *Bunocephalus serranoi* from the late Miocene; (B) stem calibration of Clariidae, based on a fossil from the lower Eocene.

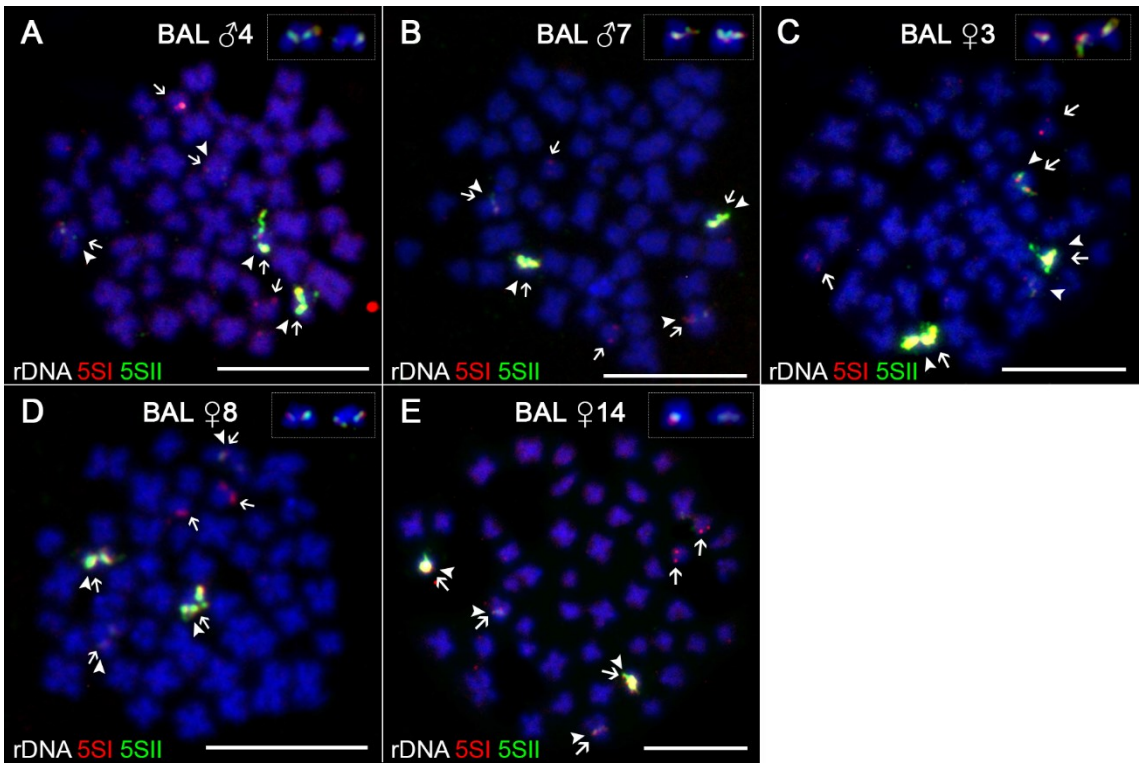

Fig. S8 Metaphases of selected *B. aloikae* individuals after FISH with the 5S rDNA variants I and II. 5S rDNA variant I (red; arrow); variant II (green; arrowhead). Insets: chromosome pair with the strong 5S rDNA signals, after shorter exposition time, for better assesment of signal location. Note that both 5S rDNA variants colocalize on one pair with strong signals and one pair with tiny signals. 5S rDNA var. I exhibits additional signals on one or two another chromosomes. Scale bar = 10 μm.

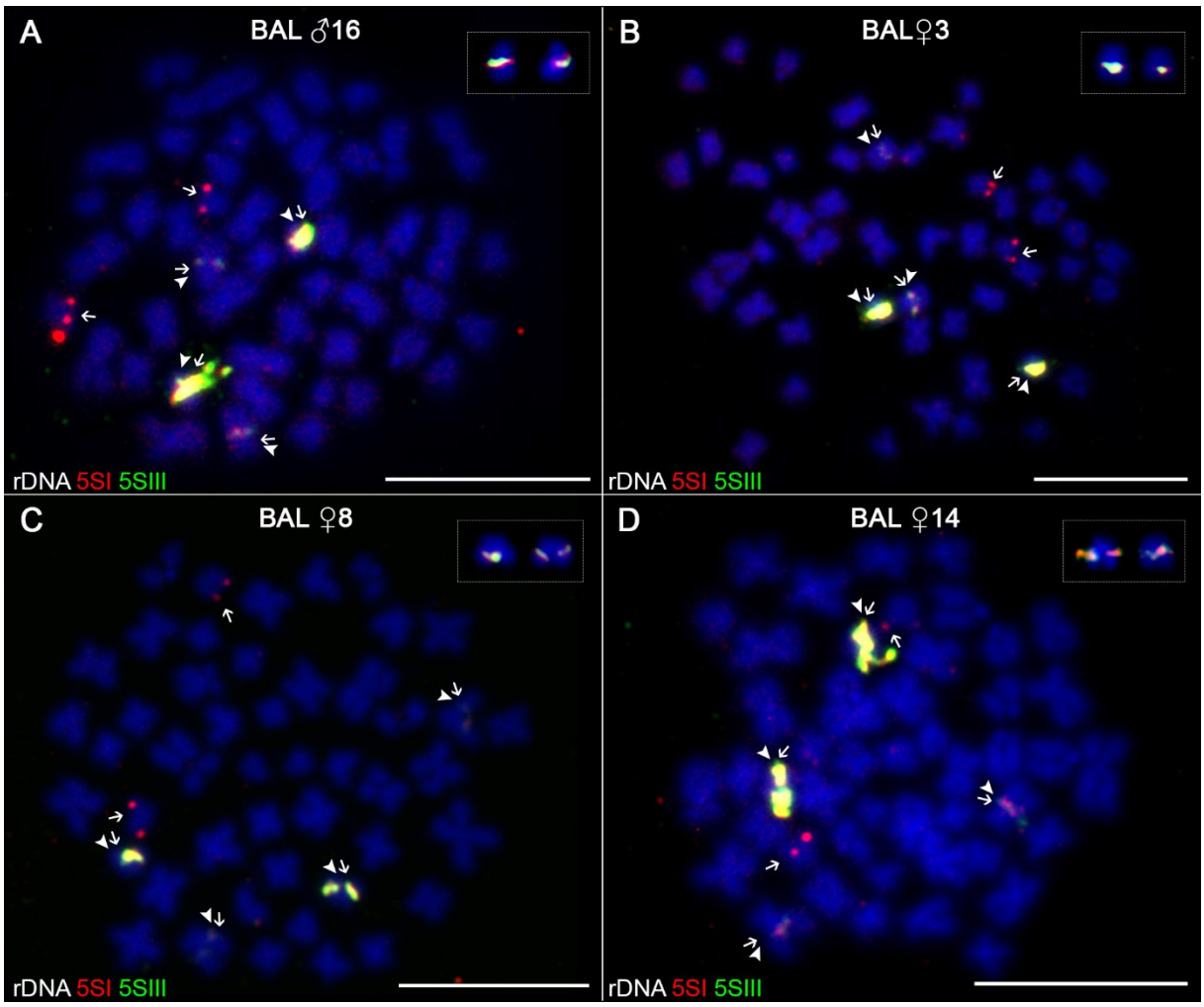

Fig. S9 Metaphases of selected *B. aloikae* individuals after FISH with the 5S rDNA variants I and III. 5S rDNA variant I (red; arrow); variant III (green; arrowhead). Insets: chromosome pair with the strong 5S rDNA signals, after shorter exposition time, for better assesment of signal location. Note that both 5S rDNA variants colocalize on one pair with strong signals and one pair with tiny signals. 5S rDNA var. I exhibits additional signals on two another chromosomes. Scale bar = 10 μm.

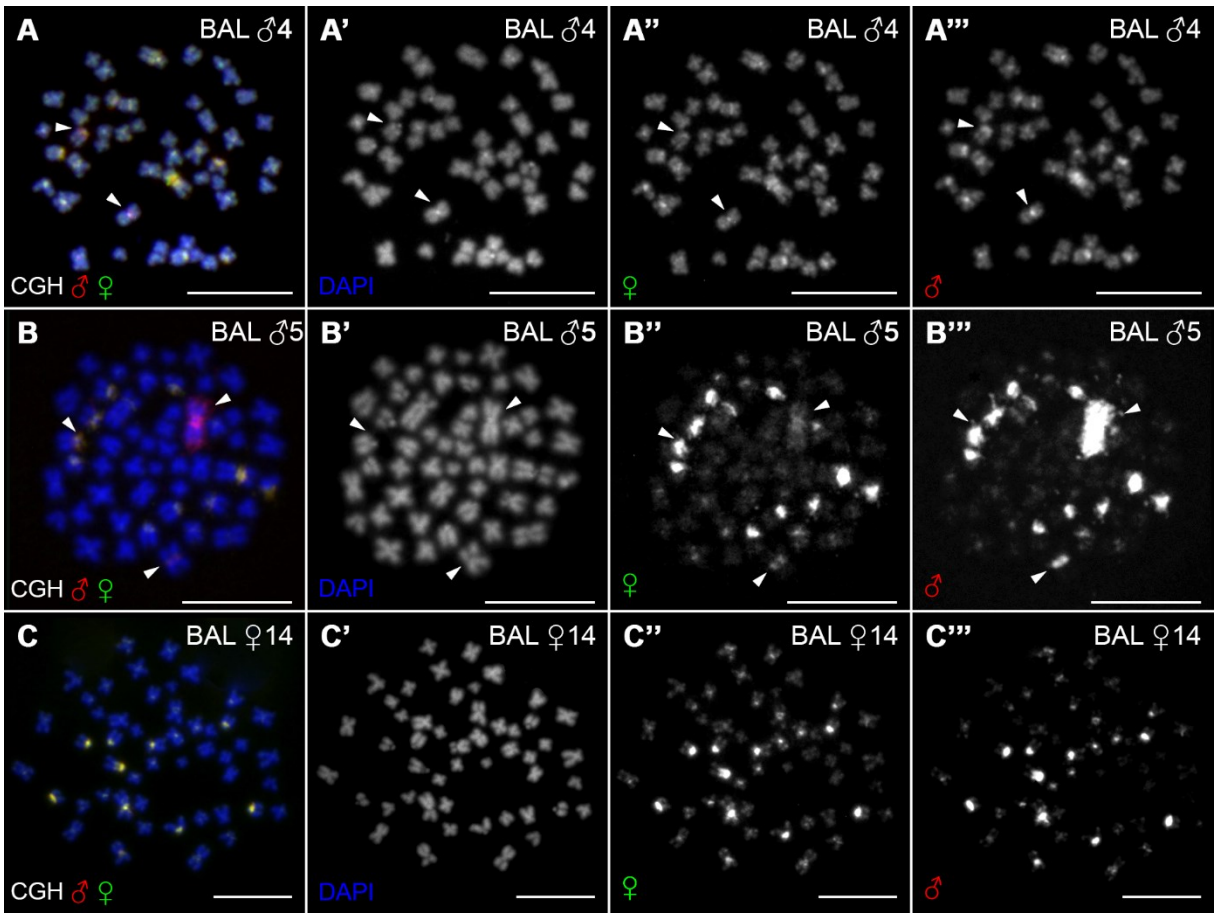

Fig. S10 Selected results from comparative genomic hybridisation in analysed *B. aloikae* males — extended file with separated channels. First column: merged images of both genomic probes and DAPI; Second column: DAPI images (blue); Third column: hybridisation patterns generated by the female genomic probe (green); Fourth column: hybridisation patterns generated by the. male genomic probe (red). Scale bar = 10 μm.

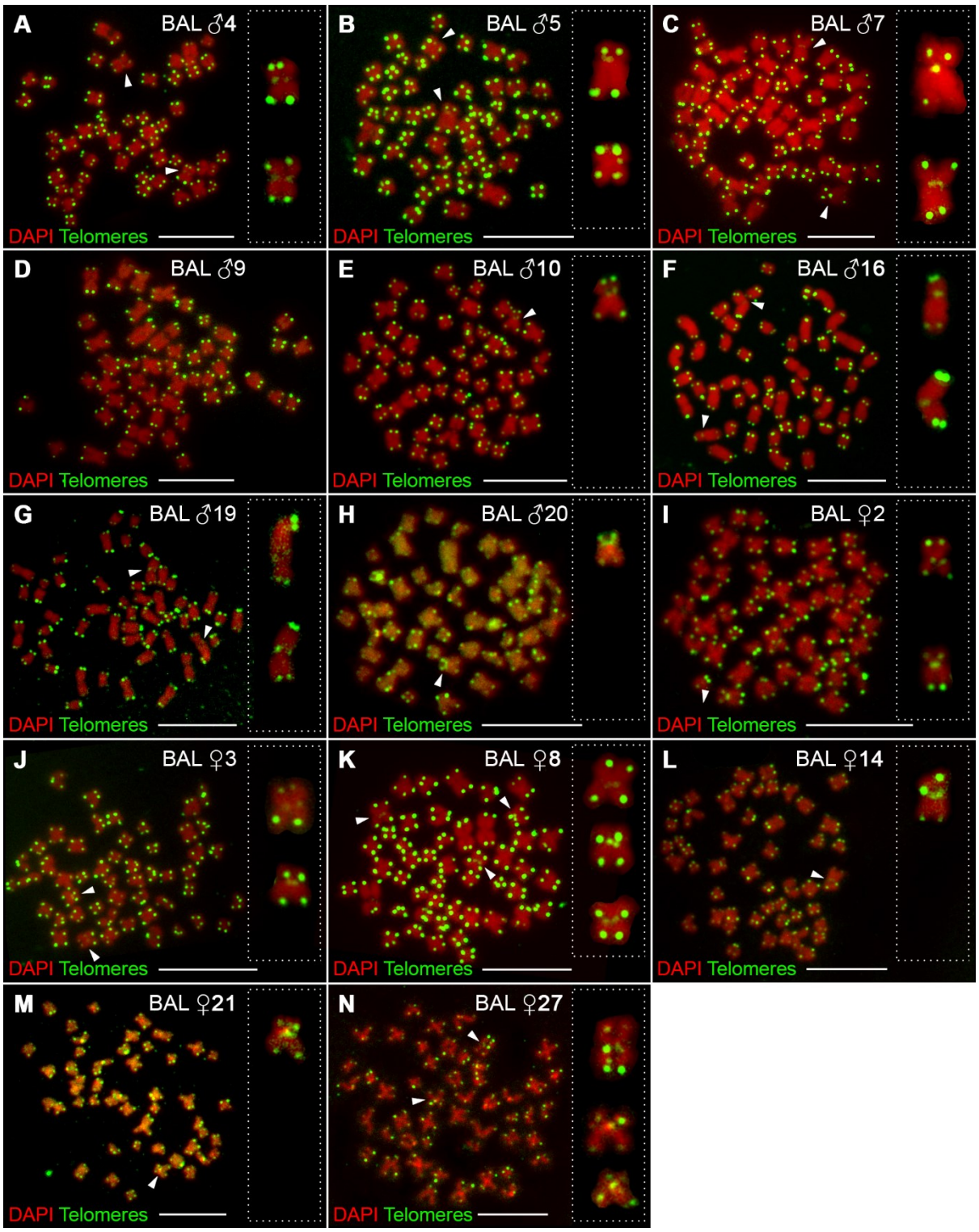

Fig. S11 Metaphases of *Bunocephalus aloikae* individuals after FISH with telomeric probe. For better contrast, pictures were pseudocolored in green (telomeric repeat probe) and red (DAPI). Arrows indicate interstitial telomeric sites (ITSs) that are also highlighted in the brackets. Scale bar = 10.

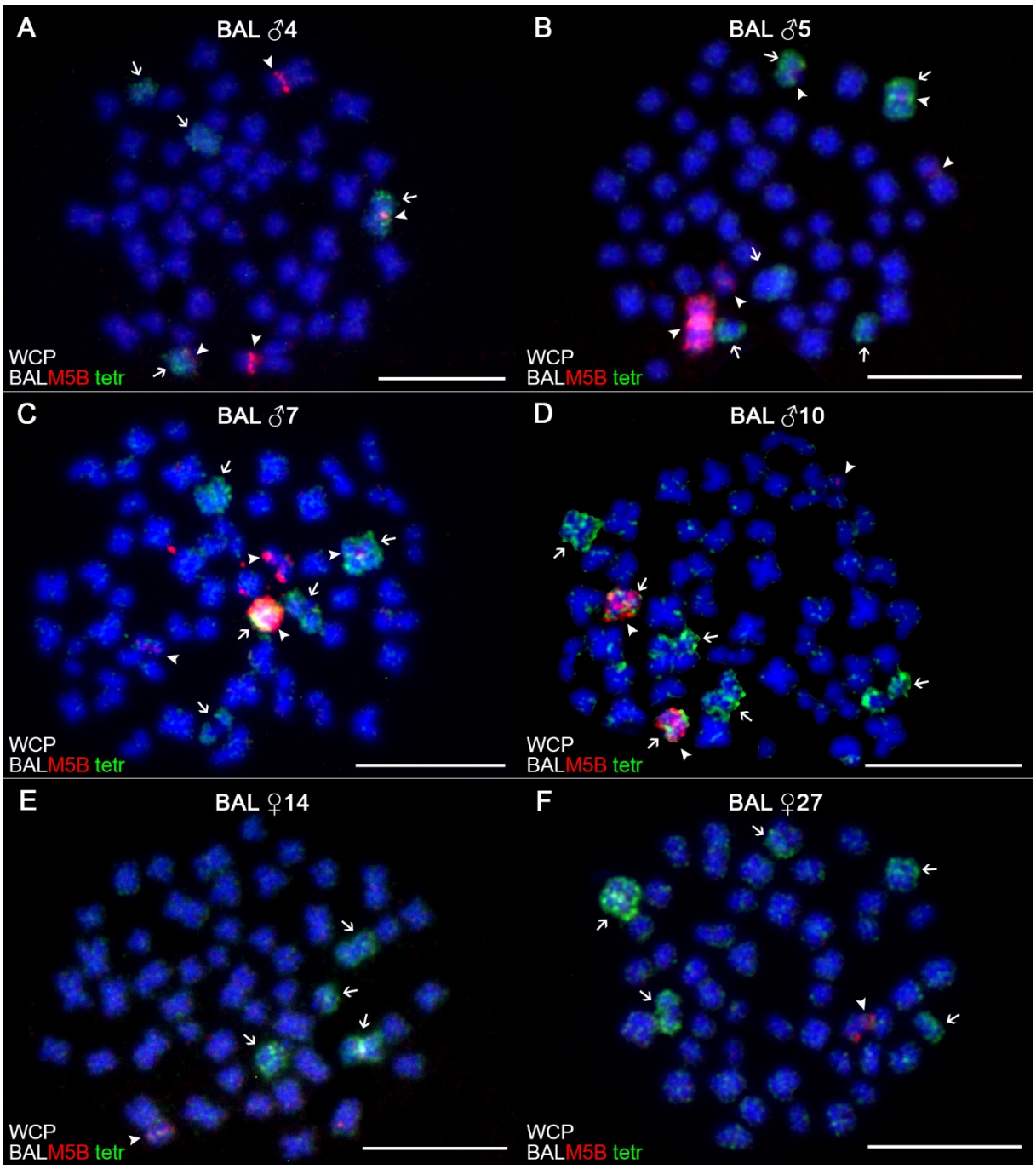

Fig. S12 Metaphases of *Bunocephalus aloikae* male individuals 4, 5, 7, 10 and female individuals 14 and 27 after WCP with BAL-M5B probe. The probe (red, full arrowhead) is derived from single large DAPI-positive metacentric chromosome found in the male BAL-M5, while the probe BAL-tetr (green, arrow) is derived from male BAL-M4.

Text S1: 5S and 18S rDNA probe preparation

The 5S rDNA fragments were PCR-amplified using previously optimized primers and thermal profiles [4–6]. The resulting PCR products were purified using NucleoSpin Gel and PCR Clean-up (Macherey-Nagel), cloned into a pDrive vector (Qiagen), and positive bacterial colonies were subsequently used for plasmid isolation and sequencing (in both strands) by Macrogen company (Netherlands). This workflow including the subsequent assembly of chromatograms from obtained sequences and sequence alignment followed essentially Sember et al. [6]. The content of resulting consensus sequences was verified using NCBI BLAST/N analysis [7] and selected clones were used for a FISH probe preparation. The probe composition and FISH conditions followed Sember et al. [6] with slight modifications specified in Štundlová et al. [8].

The 18S rDNA probe was generated in two steps: (i) non-labelling PCR amplification using the previously described primers [9] from a verified 18S rDNA clone and (ii) nick translation (incubation time 1 h 40 min at 15 °C) of the amplified 18S rDNA product using Nick Translation Mix (Abbott Molecular, IL, USA) and digoxigenin-16-dUTP (Roche, Mannheim, Germany). 5S rDNA fragments (particularly sequence variant I; see the Results section in the main text) were instead labelled by PCR using a nucleotide mix containing biotin-dUTP (Roche). In a subset of experiments aimed to simultaneously map 5S rDNA variant I with other variants; those other variants were labelled with digoxigenin-dUTP.

Text S2: Individual-specific cytogenetic patterns

BAL-M4; 2n=48 (Fig. 4A-D; A+D and B+C sequential)
This male individual which possessed 2n=48 chromosomes served as the source for preparation of the two (resp. three) WCP probes (BAL-tetr, BAL-meta, and BAL-stl) as well as for meiotic analyses. The reverse FISH with the BAL-tetr probe revealed four chromosomes of distinct morphology. The BAL-meta probe entirely painted one large metacentric and one large subtelocentric chromosome (Fig. 4A). The application of the probe derived from the large submetacentric element, BAL-stl, confirmed the painting pattern (i.e. full overlap with the BAL-meta probe). BAL-M5B (Fig. S12) produced signals on four chromosomes, two of them colocalized with members of the tetravalent. The 18S rDNA probe produced signals on two morphologically different chromosomes; these chromosomes are members of the tetravalent. 5S rDNA var. I probe displayed two strong and four considerably weaker signals; none of these chromosomes were painted by either of the WCP probes. The complement displayed 10 (7 strong, 3 weak) CMA_3^+ signals, especially in DAPI-negative chromosomal gaps, 18S rDNA sites and BAL-meta positive chromosomes. C-banding showed more pronounced signals particularly in the 18S rDNA sites. The telomeric probe revealed two ITSs (Fig. S11). CGH uncovered in this and most of all other males two remarkable male-enriched signals, both on chromosomes included in the formation of tetravalent (compared to BAL-tetr patterns) (Fig. 7). These male-enriched signals overlapped with 18S rDNA sites (Fig. 8). Meiotic data are also available for this male individual (Fig. 9); the BAL-tetr probe indicates a single object formed by four chromosomes. Additionally, we performed the labelling with the BAL-M5B probe – it marks four chromosomes, two of which colocalize with the tetravalent, while the remaining two mark a metacentric pair (Fig. S12).

BAL-M5 2n=50 including 1 B chromosome (Fig. 4E-H; F and H sequential)
The complement was composed of 2n=50 chromosomes, including one large B chromosome. From this B chromosome we constructed additional painting probe designated as BAL-M5B. BAL-tetr probe indicated five chromosomes differing in their sizes and morphology (Fig. S12). In one

of these chromosomes (large submetacentric) the probe stained only a portion of q-arms. BAL-meta marked three chromosomes – one large submetacentric and two smaller chromosomes (submetacentric and subtelocentric). In meiosis (Fig. 9C) the BAL-tetr probe stained two objects – a tetravalent and a part of a bivalent – and the BAL-meta probe stained one object – a trivalent. The BAL-M5B probe (Fig. S12) produced signals on five chromosomes; two of them were part of the tetravalent and were weakly labelled in their centromeres. The same probe further stained the large heterochromatic metacentric B chromosome (from which the probe originates) and parts of two other chromosomes: part of p-arms of large submetacentric and terminal portion of q-arms of an acrocentric chromosome. 18S rDNA probe produced signals on two morphologically distinct chromosomes, members of a tetravalent. 5S var. I probe displayed two strong and four considerably weaker signals; none of these chromosomes was painted by either painting probe. Chromomycin A_3 stained 12 chromosomes (8 strong and 4 weaker signals) including 18S rDNA regions and a large metacentric chromosome. C-banding displayed, besides many pericentromeric signals, enlarged signals in the 18S rDNA-labelled regions and strong staining was shown on the large B chromosome (but with much less intensity compared to the other B chromosomes of the remaining herein studied individuals). In the Fig. 4E note that part of the tetravalent translocated to another chromosome (red arrowhead), present in a single copy. The B chromosome is here strongly DAPI-positive. This B chromosome is also remarkable for its strong male-specific CGH signal (see Fig. 7). Fig. 4G: This CMA_3-stained metaphase was recycled after WCP (WCP not shown). Fig. 4H: The B chromosome is here less heterochromatic than in other individuals (compare with Fig. 4L, T) and also WCP probes stained it much less intensely (Fig. 4E). The telomeric probe revealed two ITSs (Fig. S11).

BAL-M7; 2n=51 including 1 B chromosome (Fig. 4I-L; full sequence)
This male had the highest chromosome count within the sampling. BAL-tetr marked four chromosomes with distinct morphology. BAL-meta marked three chromosomes – one large submetacentric and two smaller chromosomes (submetacentric and acrocentric). The submetacentric chromosome additionally possessed a DAPI-negative centromeric region. Both probes colocalized on the B chromosome (orange signal). Meiotic data (Fig. 10) showed a clear evidence of unequal segregation of B chromosomes, with none-to-two elements in sister metaphases II. The B chromosome(s) did not pair with standard (A) chromosomes. Mapping of the BAL-M5B probe (Fig. S12) revealed signals on three chromosomes: it entirely labelled the B chromosome and produced faint signals on two additional elements morphologically resembling those marked by the BAL-meta probe (large submetacentric and telocentric chromosome); no signal was found on the tetravalent. The 18S rDNA probe labelled two morphologically distinct chromosomes that colocalized with the tetravalent-forming linkage groups. Additionally weak signals were observed to scatter across the B chromosome. 5S rDNA var. I probe produced two strong signals and three weaker ones; none colocalized with our painting probes. CMA_3 staining revealed 8 strong and 4 weak signals. A visible GC+/AT- segment was amplified on the large submetacentric chromosome. Strong signals were visible to colocalize with 18S rDNA signals, while no CMA_3^+ signals were observed on the B chromosome or on chromosomes carrying 5S rDNA. Chromosomes marked by the BAL-meta probe possessed a strong CMA_3^+ signal. Besides pericentromeric regions, remarkable heterochromatic blocks were present in the 18S rDNA regions and the B chromosome was completely heterochromatinized. CGH revealed a remarkable male-enriched signal on the presumed B chromosome (Fig. 7). The telomeric probe revealed two ITSs (Fig. S11).

BAL-M9; 2n=49 (Fig. 4M-P; full sequence)
BAL-tetr marked four chromosomes with distinct morphology, BAL-meta marked two chromosomes (one large metacentric and one large submetacentric). The submetacentric chromosome additionally possessed DAPI-negative centromere. This individual bore 18S signals on morphologically similar chromosomes. The probe for 5S rDNA var. I produced a standard pattern, i.e. two strong signals and four weaker ones; none of these colocalized with either painting probe. CMA_3 revealed five strong and five weak signals. A remarkable GC-rich/DAPI-negative segment was amplified on the large submetacentric chromosome. A strong signal was visible on chromosomes with 18S rDNA, while no signal was observed on the B chromosomes or chromosomes with 5S rDNA. Chromosomes marked by the BAL-meta probe exhibited a strong signal. The telomeric probe revealed no ITSs (Fig. S11).

BA-M10; 2n=50 including 2 B chromosomes (Fig. 4Q-T; R-T sequential)
BAL-tetr painted four chromosomes with different morphology; one of these chromosomes is a metacentric where only one of the two arms was painted. BAL-meta stained three chromosomes (one large submetacentric and two smaller chromosomes – submetacentric and acrocentric). Out of them, the submetacentric chromosome did not carry any BAL-meta signal in the (peri)centromeric region. This individual is remarkable for the presence of two B chromosomes of slightly different morphologies (acrocentric-to-subtelocentric). The BAL-M5B probe (Fig. S12) produced signals on three chromosomes – it entirely painted two Bs and produceda a faint signal on the p-arms of one large submetacentric element with DAPI-negative centromere. 18S rDNA probe revealed signals on two apparently homologous chromosomes (of the same size and morphology). 5S var. I probe produced two strong and three weak signals; none of them placed on chromosomes stained by the set of painting probes. CMA_3 revealed seven strong and three weak signals. The strong ones overlapped with 18S rDNA signals and some other were placed on three chromosomes painted also by the BAL-meta probe, including particularly the DAPI-negative centromere of one of these chromosomes. Pronounced blocks of constitutive heterochromatin overlapped with 18S rDNA sites and B chromosomes were entirely heterochromatinized. CGH (Fig. 7E) further revealed two remarkably male-enriched signals, most likely on the B chromosomes based on their morphology. The telomeric probe revealed an ITS on a single chromosome (Fig. S11).

BAL-M16; 2n=49 (Fig. 5A-D; full sequence)
BAL-tetr probe stained four chromosomes one of which is large metacentric and the rest are subtelocentrics-to-acrocentrics of medium or small size. BAL-meta probe stained three chromosomes, each of them of different size and morphology (large subtelocentric, medium metacentric, small acrocentric). 18S rDNA signals rested in the pericentromeric regions of two markedly different chromosomes – large metacentric and rather small subtelocentric (both, again, stained by the BAL-tetr probe). 5S rDNA probes produced two robust and four tiny signals. CMA_3 produced seven clear (peri)centromeric signals. C-bands were remarkable in the two 18S rDNA regions and then they also occupied pericentromeric regions of majority of chromosomes. The telomeric probe revealed two ITSs (Fig. S11).

BAL-M19; 2n=49 (Fig. 5E-H; full sequence)
BAL-tetr stained four chromosomes: two large metacentrics and two small acrocentrics (the possibility to arrange these four chromosomes into homologous pairs suggests perhaps the original situation before the rearrangement between these linkage groups). BAL-meta painted three chromosomes, each of different morphology and size (large sm/st, large submetacentric with apparent DAPI-/CMA_3^+ pericentromeric region, and small acrocentric element). A pair of 18S

rDNA signals occupied (peri)centromeric region of two homologous large metacentrics (in line with the WCP pattern). The 5S rDNA probe produced two robust and four tiny signals. CMA_3 signals were not clearly visible after repeated treatments in this individual, but the overall signal pattern was generally consistent with the range observed in other individuals. C-bands were remarkable in two 18S rDNA regions and then they also occupied pericentromeric regions of majority of chromosomes. The telomeric probe revealed two ITSs (Fig. S11).

BAL-M20; 2n=50 (Fig. 5I-L; J-L sequential)
BAL-tetr painted four chromosomes, one pair of metacentrics and two nonhomologous chromosomes (large metacentric and small acrocentric). BAL-meta stained three chromosomes – one large metacentric and two st-a elements. In meiosis (Fig. 9G) BAL-tetr stained one object – a tetravalent – and BAL-meta also stained a single object – a trivalent. 18S rDNA was placed on the large metacentric and medium-sized acrocentric chromosome (both signals at pericentromeric position). 5S rDNA probe produced six signals, two strong and four tiny. Interestingly, two of them were placed in the pericentromeric region of two metacentrics. CMA_3 stained strongly five chromosomes (18S rDNA regions and chromosomes stained by BAL-meta probe) and five more carried weaker signals. Stronger C-bands were visible only in 18S rDNA regions. This individual was remarkable for a single chromosome with male-enriched CGH signal (Fig. 7; all other males possessed two signals and additional ones on B chromosomes if present). The telomeric probe revealed an ITS on a single chromosome (Fig. S11).

BAL-F2; 2n=49 (Fig. 5M-P; full sequence)
BAL-tetr painted five chromosomes with the following morphologies: one large and one medium-sized metacentric, two medium-sized acrocentrics and the terminal part of one large metacentric element. 18S rDNA was carried by a one large metacentric and one acrocentric chromosome. BAL-meta probe stained three chromosomes – one large submetacentric, one medium-sized submetacentric and one rather small acrocentric. 5S rDNA probe showed a standard pattern (6 signals of which two were strong). CMA_3 showed five prominent and six weaker signals. Of the strong ones, one encompassed the centromeric region of the remarkably large submetacentric element (labelled by BAL-tetr); this centromeric region was otherwise not heterochromatinized after C-banding. More pronounced C-bands were located only around the two 18S rDNA sites. Interestingly, This female is remarkable for its CGH pattern: only in this female CGH revealed two male-enriched signals, matching thus the pattern found in the majority of males (Fig. 7). The telomeric probe revealed two ITSs (Fig. S11).

BAL-F3; 2n=50 (Fig. 5Q-T; full sequence)
Three acrocentrics and one submetacentric element were painted by the BAL-meta probe. Four chromosomes were stained by the BAL-tetr probe, each of them of different size (two metacentrics, two acrocentrics). Larger metacentric and larger acrocentric element carried each an 18S rDNA site. 5S rDNA displayed a standard pattern (6 signals of which two were strong). CMA_3 showed six prominent and five weaker signals. C-banding pattern, besides standard pericentromeric occupation, was more remarkable only around the 18S rDNA site on the acrocentric chromosome pair. The telomeric probe revealed two ITSs (Fig. S11).

BAL-F8; 2n=47 (Fig. 6A-D; B-C sequential)
This female had the lowest recorded 2n within our sampling. BAL-tetr probe stained a pair of subtelocentric chromosomes and only short arms of two homologous large submetacentric chromosomes. These submetacentrics had pericentromeric 18S rDNA site as well as a notable C-band in this region. The 5S rDNA probe showed only five signals; the sixth, if present, was

indistinguishable. CMA_3 showed six stronger and five weaker signals. The telomeric probe revealed three ITSs (Fig. S11).

BAL-F14; 2n=49 (Fig. 6E-H; F-H sequential)
BAL-tetr painted four chromosomes, each of different morphology and size. Out of them, one metacentric and one acrocentric element bore 18S rDNA site along with more pronounced C-bands. BAL-meta probe painted three chromosomes, each of different size and morphology. BAL-M5B (Fig. S12) produced signal on the p-arms of a single large submetacentric element. FISH with 5S rDNA revealed a standard pattern (6 signals of which two are strong). CMA_3 showed 10 signals of similar intensity. The telomeric probe revealed an ITS on a single chromosome (Fig. S11).

BAL-F21; 2n=49 (Fig. 6I-L; full sequence)
BAL-tetr probe produced signals on four chromosomes – it entirely painted two homologous metacentrics and one acrocentric chromosome, and stained one arm of the largest unpaired metacentric chromosome. This arm also encompassed one of the two 18S rDNA signals, colocalized with a pronounced C-band; the second 18S rDNA site was located in the (peri)centromere of one metacentric homolog. Only five 5S rDNA signals (two strong, three weak) were visible in this individual. CMA_3 unveiled six prominent and four weaker signals. The telomeric probe revealed an ITS on a single chromosome (Fig. S11).

BAL-F27; 2n=49 (Fig. 6M-P; full sequence)
The WCP probes displayed an exceptional pattern: two metacentric chromosomes had one arm painted by the BAL-tetr probe, and the second arm by the BAL-meta probe. Altogether, BAL-tetr and BAL-meta painted five and six chromosomes, respectively, none of which displayed similar shape/size. BAL-M5B (Fig. S12) produced signal on the terminal portion of q-arms of a single acrocentric chromosome. 18S rDNA sites were present on one metacentric and one acrocentric chromosome. Intriguingly, the site on the metacentric element was shifted more towards the chromosome arm, in contrast to clearly pericentromeric position recorded in other individuals. FISH with 5S rDNA revealed a standard pattern (6 signals of which two are strong). CMA_3 unveiled six prominent and four weaker signals. The telomeric probe revealed three ITSs (Fig. S11).

Text S3: Additional discussion to 5S rDNA variants and hybridization patterns

Intriguingly, our rDNA probes derived from *B. aloikae* applied to *B. coracoideus* provided patterns not fully consistent with the results reported by Ferreira et al. [10,11]. This discrepancy and the presence of multiple 5S rDNA variants revealed in the present study in *B. aloikae* highlight the shortcomings of cross-species application of the 5S rDNA probes as it might not always reveal comprehensively the complete picture of species-specific rDNA evolution. Mutliple 5S rDNA variants have been revealed in a range of teleosts and other cold-blooded vertebrates and they might represent either pseudogenes or functional copies with tissue/developmental specific roles [12-15]. While appealing, exploring this topic in detail in *B. aloikae* exceeds the scope of the present study.

Supplementary References

1. Ward RD, Zemlak TS, Innes BH, Last PR, Hebert PDN. DNA barcoding Australia's fish species. Phil Trans R Soc B. 2005;360:1847–1857. https://doi.org/10.1098/rstb.2005.1716
2. Sullivan JP, Lundberg JG, Hardman M. A phylogenetic analysis of the major groups of catfishes (Teleostei: Siluriformes) using *rag1* and *rag2* nuclear gene sequences Mol Phyl Evol. 2006;40:636–662. https://doi.org/10.1016/j.ympev.2006.05.044
3. Li C, Ortí G, Zhang G, Lu G. A pratical approach to phylogenomics: the phylogeny of ray-finned fish (Actinopterygii) as a case study. BMC Evol Biol. 2007;7:44. https://doi.org/10.1186/1471-2148-7-44
4. Martins C, Galetti PM. Chromosomal localization of 5S rDNA genes in *Leporinus* fish (Anostomidae, Characiformes). Chromosome Res. 1999;7:363-367. https://doi.org/10.1023/A:1009216030316
5. Alves-Costa FA, Martins C, de Matos FDC, Foresti F, Oliveira C, Wasko apod. 5S rDNA characterization in twelve Sciaenidae fish species (Teleostei, Perciformes): depicting gene diversity and molecular markers. Genet Mol Biol. 2008;31:303–307. https://doi.org/10.1590/S1415-47572008000200025
6. Sember A, Bohlen J, Šlechtová V, Altmanová M, Symonová R, Ráb P. Karyotype differentiation in 19 species of river loach fishes (Nemacheilidae, Teleostei): extensive variability associated with rDNA and heterochromatin distribution and its phylogenetic and ecological interpretation. BMC Evol Biol. 2015;15:251. https://doi.org/10.1186/s12862-015-0532-9
7. Altschul SF, Gish W, Miller W, Myers EW, Lipman DJ. Basic local alignment search tool. J Mol Biol. 1990;215(3):403-410. doi:10.1016/S0022-2836(05)80360-2.
8. Štundlová J, Hospodářská M, Lukšíková K, Voleníková A, Pavlica T, Altmanová M, et al. Sex chromosome differentiation via changes in the Y chromosome repeat landscape in African annual killifishes *Nothobranchius furzeri* and *N. kadleci*. Chromosome Res. 2022;30:309–333. https://doi.org/10.1007/s10577-022-09707-3
9. Cioffi MB, Martins C, Centofante L, Jacobina U, Bertollo LAC. Chromosomal variability among allopatric populations of Erythrinidae fish *Hoplias malabaricus*: mapping of three classes of repetitive DNAs. Cytogenet Genome Res. 2009;125:132–141. https://doi.org/10.1159/000227838
10. Ferreira M, Garcia C, Matoso DA, Jesus IS, Feldberg E. A new multiple sex chromosome system $X_1X_1X_2X_2/X_1Y_1X_2Y_2$ in Siluriformes: cytogenetic characterization of *Bunocephalus coracoideus* (Aspredinidae). Genetica. 2016;144:591–599. https://doi.org/10.1007/s10709-016-9927-9
11. Ferreira M, Garcia C, Matoso DA, Jesus IS, Cioffi MB, Bertollo LAC, et al. The *Bunocephalus coracoideus* species complex (Siluriformes, Aspredinidae): signs of a speciation process through chromosomal, genetic and ecological diversity. Front Genet. 2017;8:120. https://doi.org/10.3389/fgene.2017.00120
12. Rebordinos L, Cross I, Merlo A. High evolutionary dynamism in 5S rDNA of fish: state of the art. Cytogenet Genome Res 2013;141:103–113. https://doi.org/10.1159/000354871
13. Vierna J, Wehner S, Höner zu Siederdissen C, Martinez-Lage A, Marz M. Systematic analysis and evolution of 5S ribosomal DNA in metazoans. Heredity. 2013;111:410–421. https://doi.org/10.1038/hdy.2013.63
14. Locati MD, Pagano JF, Ensink WA, Van Olst M, Van Leeuwen S, Nehrdich U, et al. Linking maternal and somatic 5S rRNA types with different sequence-specific non-LTR retrotransposons. RNA. 2017;23:446–456. https://doi.org/10.1261/rna.059642.116

15. Davidian AG, Dyomin AG, Galkina SA, Makarova NE, Dmitriev SE, Gaginskaya ER. 45S rDNA repeats of turtles and crocodiles harbor a functional 5S rRNA gene specifically expressed in oocytes. Mol Biol Evol. 2022;39:msab324. https://doi.org/10.1093/molbev/msab324